

Characterization of little skate (*Leucoraja erinacea*) recombinant transthyretin:
Zinc-dependent 3,3',5-triiodo-l-thyronine binding

メタデータ	言語: eng 出版者: 公開日: 2016-04-19 キーワード (Ja): キーワード (En): 作成者: Suzuki, Shunsuke, Kasai, Kentaro, Yamauchi, Kiyoshi メールアドレス: 所属:
URL	http://hdl.handle.net/10297/9350

1 Characterization of little skate (*Leucoraja erinacea*) recombinant transthyretin:
2 zinc-dependent 3,3',5-triiodo-L-thyronine binding

3
4 Shunsuke Suzuki ^{a†}, Kentaro Kasai ^{a†}, Kiyoshi Yamauchi ^{a,b*}

5
6 ^aDepartment of Biological Science, Graduate School of Science, Shizuoka University, Shizuoka 422-8529,
7 Japan

8 ^bGreen Biology Research Division, Research Institute of Green Science and Technology, Shizuoka
9 University, Shizuoka 422-8529, Japan

10
11
12 †Equally contributing author.

13 *Corresponding author. Green Biology Research Division, Research Institute of Green Science and
14 Technology, Shizuoka University, Shizuoka 422-8529, Japan. Tel.: +81 54 238 4777, fax: +81 54 238
15 0986.

16 *E-mail address:* fgyfm536@gmail.com (S. Suzuki), mitsuya59451192@gmail.com (K. Kasai),
17 sbkyama@ipc.shizuoka.ac.jp (K. Yamauchi).

18
19 *Abbreviations:* BSA, bovine serum albumin; EDTA, ethylenediaminetetraacetic acid; HIU,
20 5-hydroxyisourate; HIUHase, 5-hydroxyisourate hydrolase; HPLC, high-performance liquid
21 chromatography; IC₅₀, 50% inhibitory concentration; ICP-OES, inductively coupled plasma optical
22 emission spectroscopy; IPTG, isopropyl β-D-1-thiogalactopyranoside; K_d, dissociation constant; MBC,
23 maximum binding capacities; PAGE, polyacrylamide-gel electrophoresis; reverse T3 or rT3,
24 3,3',5'-triiodo-L-thyronine; PCR, polymerase chain reaction; SDS, sodium dodecyl sulfate; T3,
25 3,3',5-triiodo-L-thyronine; T4, L-thyroxine; TH, thyroid hormone; TTR, transthyretin.

28 **Abstract**

29 Transthyretin (TTR) diverged from an ancestral 5-hydroxyisourate hydrolase (HIUHase) by gene
30 duplication at some early stage of chordate evolution. To clarify how TTR had participated in the thyroid
31 system as an extracellular thyroid hormone (TH) binding protein, TH binding properties of recombinant
32 little skate *Leucoraja erinacea* TTR was investigated. At the amino acid level, skate TTR showed 37–46%
33 identities with the other vertebrate TTRs. Because the skate TTR had a unique histidine-rich segment in the
34 N-terminal region, it could be purified by Ni-affinity chromatography. The skate TTR was a 46-kDa
35 homotetramer of 14.5 kDa subunits, and had one order of magnitude higher affinity for
36 3,3',5-triiodo-L-thyronine (T3) and some halogenated phenols than for L-thyroxine. However, the skate
37 TTR had no HIUHase activity. Ethylenediaminetetraacetic acid (EDTA) treatment inhibited [¹²⁵I]T3
38 binding activity whereas the addition of Zn²⁺ to the EDTA-treated TTR recovered [¹²⁵I]T3 binding activity
39 in a Zn²⁺ concentration-dependent manner. Scatchard analysis revealed the presence of two classes of
40 binding site for T3, with dissociation constants of 0.24 and 17 nM. However, the high-affinity sites were
41 completely abolished with 1 mM EDTA, whereas the remaining low-affinity sites decreased binding
42 capacity. **The number of zinc per TTR was quantified to be 4.5–6.3. Our results suggest that skate TTR has**
43 **tight Zn²⁺-binding sites, which are essential for T3 binding to at least the high-affinity sites. Zn²⁺ binding to**
44 **the N-terminal histidine-rich segment may play an important role in acquisition or reinforcement of TH**
45 **binding ability during early evolution of TTR.**

46

47 *Keywords:* transthyretin, thyroid hormone, divalent cation, endocrine disruption, 5-hydroxyisourate
48 hydrolase, *Leucoraja erinacea*

49

50

51

52

53 **1. Introduction**

54 Plasma thyroid hormone (TH) binding proteins ensure the adequate distribution of THs in circulation
55 to tissues. Plasma TH-binding proteins consist of thyroxine-binding globulin, transthyretin (TTR) and
56 albumin (Robbins, 1996), all of which appeared during vertebrate evolution. However, the phylogenetic
57 distribution of these TH-binding proteins is species-specific. TTR acts as a major TH-binding protein in
58 some fish (Santos and Power, 1999; Yamauchi et al., 1999). In addition, lipoproteins and albumin are also
59 known as major TH-binding proteins with low affinity for THs in immature salmonids (Cyr and Eales,
60 1992; Richardson et al., 2005). However, there is a lack of information about the TH binding properties of
61 TTR from lower vertebrates such as elasmobranchs.

62 Chondrichthyes or cartilaginous fishes are an extant group that diverged from the earliest
63 gnathostomes about 395 million years ago (Benton, 2005). Most elasmobranchs, including skates, have
64 important ecological positions as top- or meso-predators within marine food webs. However, little is known
65 about the non-natural ligands of skate TTR, including agricultural, industrial, and pharmaceutical chemicals
66 that may be expected to displace THs from TTR and act as endocrine disruptors.

67 The TTR gene arose from an ancestral 5-hydroxyisourate hydrolase (HIUHase) gene by
68 neo-functionalization after gene duplication at some early stage of chordate evolution (Ramazzina et al.,
69 2006; Zanotti et al., 2006). Because this event occurred around the time that the thyroid system was
70 established, the ancestor of TTR is likely to have acquired the ability to bind TH soon after gene
71 duplication. Intriguingly, only two point mutations in zebrafish or amphioxus HIUHases resulted in the
72 acquisition of TH binding activity and the loss of 5-hydroxyisourate (HIU) hydrolysis activity (Cendron et
73 al., 2011; Li et al. 2013).

74 The N-terminal region of TTR forms a random-coiled structure with high conformational flexibility
75 (Hamilton et al., 1993), and has important roles in the specificity and affinity of TH binding (Prapunpoj et
76 al., 2006). It has been proposed that the N-terminal region has evolved from a longer and more
77 hydrophobic region in lower vertebrates to a shorter and more hydrophilic region in eutherians, by
78 unidirectional changes (Aldred et al., 1997; Prapunpoj et al., 2000), with functional changes in TH-binding
79 specificity from for 3,3',5-triiodo-L-thyronine (T3) to for L-thyroxine (T4) (Yamauchi et al., 1993; Chang
80 et al., 1999). Through the survey of several expressed sequence tag and genome databases of elasmobranch

81 fishes, we found TTR cDNA in the little skate *Leucoraja erinacea* database (<http://skatebase.org>), and
82 noticed that such unidirectional changes may not be true for the skate TTR. Because the skate TTR has a
83 highly hydrophilic stretch containing four histidine residues in the N-terminal region as if the skate TTR
84 has a histidine tag. From this unique structure we supposed that functional analyses of the TTR gene
85 superfamily in primitive gnathostomes may provide a good model for understanding the processes of
86 neo-functionalization found in duplicated genes.

87 As a first step towards elucidating how TTR has participated in the thyroid system as a TH-binding
88 protein during vertebrate evolution, we investigated TH binding properties and HIUHase activity of the
89 recombinant skate TTR.

90

91

92 **2. Materials and Methods**

93 *2.1. Reagents*

94 3,3' [¹²⁵I],5-Triiodo-L-thyronine (81 TBq/mmol, carrier free) was purchased from PerkinElmer
95 (Waltham, MA, USA). 3,3',5-Triiodo-L-thyronine, T4, D-T3, 3,3',5'-triiodo-L-thyronine (reverse T3 or
96 rT3), 3,3',5-triiodothyroacetic acid, 3,3',5,5'-tetraiodothyroacetic acid, diiodo-L-tyrosine,
97 monoiodo-L-tyrosine, benzo[*a*]pyrene and pentachlorophenol were obtained from Sigma-Aldrich (St. Louis,
98 MO, USA). Bisphenol A, 2,4,6-triiodophenol, 2,4,6-tribromophenol, 2,4,6-trichlorophenol,
99 pentabromophenol, *o*-*t*-butylphenol, mirex, malathion (diethyl
100 2-dimethoxyphosphinothioylsulfanylbutanedioate, analytical standard), benzophenone, *n*-butylbenzyl
101 phthalate, bis(2-ethylhexyl) adipate, bis(2-ethylhexyl) phthalate, dicyclohexyl phthalate, di-*n*-butyl
102 phthalate, tributyltin (IV) chloride, α -benzoepin (α -endosulfan;
103 6,7,8,9,10,10-hexachloro-1,5,5a,6,9,9a-hexahydro-6,9,10-methano-2,4,3-benzodiazepine), dicofol (Kelthane,
104 2,2,2-trichloro-1,1-bis(4-chloro-phenyl)ethanol, analytical standard), urea, *Candida* sp. uricase and
105 trimethylamine N-oxide were purchased from Wako Pure Chemical Industries (Osaka, Japan).
106 3,3',5,5'-Tetrabromobisphenol A, 3,3',5,5'-tetrachlorobisphenol A and 3,5-diiodo-L-thyronine were from
107 Tokyo Chemical Industry (Tokyo, Japan). 2,4-Dichlorophenoxyacetic acid, 4-nonylphenol, di-2-ethyl
108 phthalate and 2,4-dinitrophenol were purchased from Kanto Chemicals (Tokyo, Japan). Isopropyl

109 β -D-1-thiogalactopyranoside (IPTG) was obtained from Nacalai Tesque (Kyoto, Japan). 2-Isopropylphenol
110 was from Lancaster. Methoprene (isopropyl (E,E')-(RS)-11-methoxy-3,7,11-trimethyldodeca-2,4-dienoate)
111 was from Ehrenstorfer Quality (Augsburg, Germany). Ioxynil (3,5-diiodo-4-hydroxybenzotriazole, analytical
112 standard) and acetochlor (2-chloro-N-(ethoxymethyl)-N-(2-ethyl-6-methylphenyl)acetamide) were obtained
113 from Riedel-de Haën (Seeize, Germany). Ni-resins were from Bio-Rad (Ni-IMAC Profinity, Hercules, CA,
114 USA) and Invitrogen (ProBond Nickel-Chelating Resin, Carlsbad, CA, USA). Co-resin was obtained from
115 Clontech (Talon Metal Affinity Resin, Mountain View, CA, USA). All other chemicals used in this study
116 were either chromatography grade or the highest grade available and were purchased from Wako Pure
117 Chemical Industries or Nacalai Tesque.

118 All chemicals tested as endocrine disrupting chemicals were dissolved in dimethylsulfoxide or 0.5 N
119 NaOH to concentrations of 2–5 mM. These chemicals were then diluted with an appropriate buffer. For
120 TTR pull-down assay, a blank assay without proteins with solvent alone at less than 1.0% (v/v) was done.
121 The solvent did not affect the recovery of TTR in the pull-down assay. For competitive [¹²⁵I]T3 binding
122 assay, a control assay without test chemicals was performed in the presence of the solvent alone and at less
123 than 0.4% (v/v). The solvent did not affect the competitive [¹²⁵I]T3 binding assay.

124

125 2.2. Protein expression and purification

126 The skate TTR cDNA (accession no. CV221819, 607 bp) was amplified by polymerase chain reaction
127 (PCR) with sense primer 5'-GTTCATATGCCACATAGTCACGGCGACC-3' (64–83) with a recognition
128 site for *NdeI* (underlined), and antisense primer 5'-GTAGGATCCGGTTTTTCACGAGGTGTTAAG-3'
129 (468–449) with a recognition site for *BamHI* (underlined). PCR was carried out in 50 μ L of solution
130 containing 0.2 mM dNTP, 0.2 μ M of each primer, 1 ng template DNA and 1.25 U DNA polymerase
131 (PrimeSTAR HS, TAKARA, Siga, Japan), using the following protocol: 98°C (15 s), and 20 cycles of
132 98°C (10 s), 65°C (5 s) and 72°C (30 s), followed by 72°C (5 min). Amplicons (64–449) were cloned
133 between the *NdeI* and *BamHI* sites of a pET3a expression vector (Novagen, Madison, WI). Plasmids for
134 expression were transformed into *Escherichia coli* Rosetta 2(DE3)pLysS (Novagen). Bacteria were usually
135 grown in 50 mL LB medium with 50 μ g/mL ampicillin and 34 μ g/mL chloramphenicol at 37°C until the
136 absorbance at 600 nm reached 0.8. The temperature was lowered to 18°C, 0.1 mM IPTG was added, and

137 incubation was continued for 16 h. Bacteria were pelleted by centrifugation ($1,200 \times g$) and stored at -35°C
138 until used.

139 After suspending the bacterial pellet with 5 mL of homogenization buffer (1 mM imidazole, 0.3 M
140 NaCl, 50 mM sodium phosphate, pH 8.0, 1 mM benzamidine hydrochloride, and 1 mM
141 phenylmethylsulfonyl fluoride), the cells were disrupted by sonication 20 times for 10 s on ice at the range
142 of 5 (UltraS homogenizer, VP-30S, TAITEC, Saitama, Japan), and the lysate was centrifuged at $18,000 \times g$
143 for 15 min at 4°C . Recombinant proteins were isolated from the other proteins in the supernatant by nickel
144 or cobalt affinity chromatography (0.5 mL of the resin), by stepwise elution with various concentrations of
145 imidazole (5, 20, 60, 150, 250 and 500 mM) in 0.3 M NaCl and 50 mM sodium phosphate, pH 8.0. Peak
146 fractions were immediately applied to a Cellulofine GCL-2000 sf column (1.5×93 cm, Seikagaku Co.,
147 Tokyo, Japan), which had been equilibrated with 20 mM Tris, pH 7.5. Purified protein was stored in 10%
148 glycerol at -85°C for later use. The yields of the recombinant proteins were 0.6–0.8 mg/50 mL bacterial
149 culture. The recombinant rainbow trout HIUHase with three histidine residues at the N-terminal end and
150 the recombinant skate TTR were also purified by ammonium sulfate precipitation, hydrophobic interaction
151 chromatography on Phenyl Cellulofine column (1.0×10 cm, Seikagaku Co.) and then gel filtration
152 chromatography on Cellulofine GCL-2000 sf column, as described previously (Kasai et al., 2013).

153

154 2.3. Protein analyses

155 Protein concentration was measured by the micro-Lowry method (Jain et al., 2002) with bovine serum
156 albumin (BSA) as the standard. Proteins was electrophoresed on an sodium dodecyl sulfate
157 (SDS)-polyacrylamide gel (15%) (Laemmli, 1970) with molecular markers: phosphorylase b (97 kDa),
158 BSA (66 kDa), ovalbumin (45 kDa), carbonic anhydrase (30 kDa), trypsin inhibitor (20.1 kDa) and
159 α -lactalbumin (14.4 kDa). The gel was stained and proteins were visualized with Coomassie Brilliant Blue.

160 The molecular mass of TTR was estimated by high-performance liquid chromatography (HPLC) on
161 YMC-Pack Diol 120 (500×8.0 mm, YMC, Kyoto, Japan) and YMC-Guardpack Diol-12 (30×8.0 mm),
162 which were pre-equilibrated and eluted with 50 mM Tris-HCl, pH 7.5, and 140 mM NaCl, at flow rate of 1
163 mL/min at 25°C .

164

165 2.4. *Ligand binding assay using a metal chelate affinity resin (TTR pull-down assay)*

166 Iodothyronine or chemical binding was carried out by the TTR pull-down assay using a metal chelate
167 affinity resin (Kasai et al., 2013). Briefly, TTR (0.5 μ M) was incubated with iodothyronines or chemicals
168 (0.5 μ M) in 500 μ L of Tris-buffered saline, pH 7.5, for 1 h at 4°C, and the mixture was further incubated
169 with Co-resin (5 μ L bed volume) for 1 h at 4°C in a 600- μ L plastic tube using a rotator. After a brief
170 centrifugation, the TTR-ligand complex bound to the resin in the pellet was immediately recovered by the
171 addition of 20 μ L of elution buffer (500 mM imidazole, 0.3 M NaCl, and 50 mM sodium phosphate, pH
172 8.0). The TTR-ligand complex released from the resin was mixed with the same volume of 1% acetic acid
173 in methanol to extract the ligand from the complex. The mixture was agitated then centrifuged at
174 $12,000 \times g$ for 10 min at 4°C. The ligand (15 μ L) in the supernatant was analyzed by reverse phase-HPLC
175 on a C₁₈ analytical column (Mightysil RP-18 GP, 250 mm \times 4.6 mm, 5 mm particle diameter, Kanto
176 Chemical, Tokyo, Japan) with a UV detector at 254 nm, as described previously (Kasai et al., 2013). The
177 amount of the ligand was quantified by comparison with the standards (4–100 pmol), **with the lower limits**
178 **of quantitation for iodothyronines and environmental chemicals of 2.0–7.2 pmol and 6–14.2 pmol,**
179 **respectively, which were three times higher than the lower limits of detection.**

180

181 2.5. *[¹²⁵I]T3 binding assay*

182 **Unlike bony fishes, cartilaginous fishes retain a high concentration of organic osmolytes, such as urea**
183 **(300–400 mM), in their body fluids to maintain a high plasma osmolality that is similar to that in the**
184 **external environment. To counteract destabilization of proteins by urea, cartilaginous fishes also have**
185 **methylamines, e.g., trimethylamine N-oxide (Yancey, 2005). Recombinant TTR (7.5 ng/tube, 0.53 nM)**
186 **was incubated with 0.1 nM [¹²⁵I]T3 in 250 μ L of buffer (20 mM Tris, pH 7.5, 280 mM NaCl, 360 mM urea,**
187 **and 90 mM trimethylamine N-oxide) in the presence or absence of test compounds (cations, unlabeled**
188 **iodothyronines or environmental chemicals) for 1.0 h at 4°C, unless otherwise noted. In some cases,**
189 **various concentrations of TTR were pre-incubated with 1 mM ethylenediaminetetraacetic acid (EDTA).**
190 **After dilution with the buffer, TTR (0.53 nM) was used for [¹²⁵I]T3 binding assay in the presence or**
191 **absence of cations. For the Scatchard plot of T3 binding to both high-affinity and low-affinity sites, skate**
192 **TTR was incubated with 0.1 nM [¹²⁵I]T3 in the presence or absence of increasing concentrations of**

193 unlabeled T3. The dissociation constant (K_d) value for high affinity sites was expected to be 10^{-10} M from
194 this experiment. To estimate more accurately the K_d value, TTR was incubated with [125 I]T3 (0.052 to 0.4
195 nM) in the presence or absence of 5 μ M of unlabeled T3. [125 I]T3 bound to proteins was separated from
196 free [125 I]T3 by the polyethyleneglycol method (Yamauchi et al., 1993). The radioactivity of the samples
197 was measured in a gamma counter (2480 WIZARD²; PerkinElmer). The amount of [125 I]T3 bound
198 non-specifically was derived from the radioactivity of samples incubated with 5 μ M unlabeled T3. The
199 non-specific binding value was subtracted from the amount of total bound [125 I]T3 that was derived from
200 the radioactivity of samples incubated without unlabeled T3, to give the value of specifically bound
201 [125 I]T3. The K_d s and maximum binding capacities (MBCs) for T3 binding were determined from
202 Scatchard plots for a single class (Scatchard, 1949) or for two classes (Rosenthal, 1967).

203

204 2.6. Determination of the average number of divalent cations per TTR

205 TTR samples were prepared by Co-affinity chromatography and gel filtration chromatography on
206 Cellulofine GCL 2000-sf column. Alternatively, to avoid the effects of Co-resin on the metal contents of
207 TTR, TTR samples were also prepared by ammonium sulfate precipitation, hydrophobic interaction column
208 chromatography, and gel filtration column chromatography, as shown previously (Kasai et al., 2013). The
209 content of divalent cations in TTR samples (1.5 mL in 4 mM Tris, pH 7.5, 0.16–0.65 mg/mL) was
210 quantified three times by inductively coupled plasma optical emission spectroscopy (ICP-OES) (Optima
211 3300 DV, PerkinElmer) using calibration curves of zinc, copper, nickel, cobalt and iron standards (0, 0.01,
212 0.05, 0.1, 0.5, 1.0, 5.0 mg/L in 0.1 mol/L HNO₃) (Wako). The lower limits of quantitation were 0.011
213 mg/mL, and the lower limits of detection were 0.002 mg/mL.

214

215 2.7. HIU hydrolysis assay

216 HIU hydrolysis assay was conducted according to the previous method (Kasai et al., 2013). Enzyme
217 activity was measured at 25–27°C by following the decrease in absorbance at 312 nm as HIU was
218 hydrolyzed (Lee et al., 2005). 5-Hydroxyisourate was generated *in situ* by the addition of 50 μ L of 0.32 μ M
219 uricase in 50 mM potassium phosphate buffer, pH 7.5, to 400 μ L of 100 μ M uric acid in the same buffer.
220 When the amount of HIU reached a maximum (2.4 min after starting the reaction), 10 μ L of HIUHase (2

221 μg) or TTR (2 μg) was added to the mixture in a microcuvette. Absorbance at 312 nm was immediately
222 monitored at 0.2 min intervals using a spectrophotometer (U-3210, Hitachi, Japan). **The control assay was**
223 **carried out similarly except that HIUHase or TTR solution was replaced by phosphate buffer.** As HIU is
224 not stable, **changes in absorbance at 312 nm does not reflect correctly the enzymatic hydrolysis of HIU.**
225 **Therefore,** the enzyme activity was expressed as the difference in absorbance at 312 nm between the
226 presence (spontaneous + enzymatic hydrolysis of HIU) and the absence (spontaneous hydrolysis of HIU) of
227 proteins.

228

229 2.8. Statistics

230 The data are the mean \pm standard error of the mean ($n \geq 3$), unless otherwise noted. Differences
231 between groups were analyzed by a one-way analysis of variance, with the Scheffe's test for multiple
232 comparisons. $P < 0.05$ was considered statistically significant.

233

234

235 3. Results

236 3.1. Comparison of TTR amino acid sequences

237 The skate TTR amino acid sequence shared 37–46% identities with the other vertebrate TTR amino
238 acid sequences shown in Fig. 1, although the skate TTR amino acid sequences shared only 24–27%
239 identities with the amphioxus and trout HIUHase amino acid sequences (data not shown). Significant
240 variations of amino acid residues were detected at the N-terminal regions, where the skate and lamprey
241 TTR had a histidine-rich segment of high hydrophilicity, HSHGDHH and HKSHEESH, respectively. Thirty
242 residues were invariant in the amino acid sequences among the 9 TTR sequences.

243

244 3.2. Molecular features of recombinant skate TTR proteins

245 Skate TTR could be purified by nickel-affinity chromatography (Fig. 2A) and gel filtration
246 chromatography. Skate TTR molecule may be a slightly compact tetramer. The molecular mass of the skate
247 TTR under native conditions was estimated to be ~46 kDa by gel filtration column chromatography (Fig.
248 2B). This value was somewhat smaller than the molecular mass of the tetramer (56.8 kDa) estimated from

249 the amino acid sequence. The molecular mass for the TTR polypeptide was 14.5 kDa on
250 SDS-polyacrylamide-gel electrophoresis (PAGE) (Fig. 2C).

251

252 *3.3. Binding of iodothyronines and environmental chemicals to recombinant skate TTR using TTR* 253 *pull-down assay*

254 3,3',5-Triiodo-L-thyronine bound to skate TTR then extracted with methanol was eluted at the same
255 retention time (11.46 min) on reverse phase-HPLC as the T3 standard, as shown previously (Kasai et al.,
256 2013). The peak of T3 was negligible when the same pull-down assay was done without TTR (blank).

257 Skate TTR exhibited high binding activity for natural ligands T3 and T4, and related compounds, with the
258 following rank order affinity: D-T3 \geq 3,3',5,5'-tetraiodothyroacetic acid, T3, T4 and
259 3,3',5-triiodothyroacetic acid \geq reverse T3 $>$ 3,5-diiodo-L-thyronine (Fig. 3A). With regard to
260 environmental chemicals (Fig. 3B), skate TTR showed binding activity for triiodophenol and ioxynil, but
261 not for benzophenone and 2,4-dinitrophenol.

262

263 *3.4. [¹²⁵I]T3 binding activity of recombinant skate TTRs*

264 *3.4.1. Effects of divalent cations*

265 To test the possibility that the skate TTR has significant affinity for metal ions, [¹²⁵I]T3 binding was
266 performed in the presence of 1 mM divalent cations. However, any cations tested did not show statistically
267 significant effects on [¹²⁵I]T3 binding (Fig. 4A). We next pre-incubated skate TTR (0.53–2640 nM) with
268 EDTA (1 mM) at various molar ratios followed by [¹²⁵I]T3 binding assay at 0.53 nM of TTR, to determine
269 the most effective molar ratio of TTR/EDTA for eliciting the chelating action of EDTA (Fig. 4B). [¹²⁵I]T3
270 binding was decreased by more than a half at the TTR pre-incubation concentration of 264 nM
271 (TTR/EDTA molar ratio of 1/3,800), and by about 90% at the TTR pre-incubation concentration of 26.4
272 nM (TTR/EDTA molar ratio of 1/38,000). Using the TTR pre-treated with 1 mM EDTA at the TTR/EDTA
273 molar ratio of 1/38,000, the effects of divalent cations (1 mM) on [¹²⁵I]T3 binding to TTR (0.53 nM) was
274 investigated (Fig. 4C). Zn²⁺, Ni²⁺ and Mn²⁺ (each 1 mM) recovered [¹²⁵I]T3 binding activity up to
275 60–90% of that of the TTR not pre-treated with EDTA. Ca²⁺ and Mg²⁺ had little effect or were not effective.
276 The effects of Fe²⁺, Co²⁺, and Cu²⁺ on [¹²⁵I]T3 binding could not be determined, because of the formation

277 of insoluble materials under our assay conditions (data not shown). Addition of 20 μM Zn^{2+} activated
278 partially [^{125}I]T₃ binding in spite of the presence of the residual EDTA (final 20 μM ; Fig 4D). [^{125}I]T₃
279 binding activity reached a plateau at more than 50 μM Zn^{2+} .

280

281 3.4.2. Competitive inhibition of [^{125}I]T₃ binding to recombinant skate TTR by iodothyronines and other 282 compounds

283 [^{125}I]T₃ binding was investigated in the presence of various concentrations of iodothyronines and their
284 related compounds (Fig. 5). The most powerful competitor was 3,3',5-triiodothyroacetic acid with 50%
285 inhibitory concentration (IC₅₀) of 1.0 ± 0.2 nM, which was two times less than the IC₅₀ for T3 (Table 1).
286 The rank order binding affinity was 3,3',5-triiodothyroacetic acid \geq T3 \geq
287 D-T3 \geq 3,3',5,5'-tetraiodothyroacetic acid > T4 > reverse T3 > 3,5-diiodo-L-thyronine > diiodo-L-tyrosine
288 and monoiodo-L-tyrosine. T3 was 13 times more potent than T4. Acetic acid analogs
289 (3,3',5-triiodothyroacetic acid and 3,3',5,5'-tetraiodothyroacetic acid) were 2-3 times more potent than the
290 corresponding iodothyronines (T3 and T4). Iodotyrosines had no affinity for skate TTR.

291 As a primary screening of environmental chemicals that interfere with [^{125}I]T₃ binding to skate TTR in
292 vitro, inhibitory effects of chemicals on [^{125}I]T₃ binding was investigated at 1 μM concentration. Out of 29
293 chemicals tested, 8 chemicals, all of which were phenolic compounds consisting of one or two phenolic
294 rings with several halogen atoms, strongly inhibited [^{125}I]T₃ binding (Fig. 6A). Phenolic compounds
295 without halogen atoms, phthalates and the other chemicals tested were not significant competitors, even if
296 they had benzene or phenolic ring(s).

297 [^{125}I]T₃ binding in the presence of varying concentrations of the eight chemicals that strongly inhibited
298 [^{125}I]T₃ binding was tested (Fig. 6B). The most effective inhibitor of [^{125}I]T₃ binding to skate TTR was
299 pentabromophenol, with an IC₅₀ of 1.4 ± 0.3 nM, which was between those for 3,3',5-triiodothyroacetic
300 acid and T3 (Table 1). The rank order binding affinity was pentabromophenol \geq triiodophenol \geq
301 pentachlorophenol \geq 3,3',5,5'-tetrabromobisphenol A \geq 3,3',5,5'-tetrachlorobisphenol A and ioxynil \geq
302 trichlorophenol and tribromophenol.

303

304 3.4.3. Kinetics of [^{125}I]T₃ binding to skate TTR

305 Scatchard plots revealed the presence of two classes of binding sites for T3 (Fig. 7), with K_{d1} and K_{d2}
306 of 0.52 ± 0.03 nM and 17 ± 3 nM, and MBC_1 and MBC_2 of 2.2 ± 1.0 pmol/ μ g protein and 19 ± 5 pmol/ μ g
307 protein, respectively. To determine more precisely the K_{d1} value, we conducted Scatchard analysis at lower
308 concentrations and within a more narrow range of [125 I]T3, which showed the K_{d1} value of 0.24 ± 0.04 nM
309 (Fig. 7 inset). In the presence of 1 mM EDTA, the Scatchard plot showed a single class of binding sites,
310 where high-affinity sites were completely abolished. The K_d value was estimated to be 21 ± 1 nM, which
311 nearly corresponded to that for the low-affinity sites of the TTR untreated with EDTA, with decreased
312 MBC value, 1.4 ± 0.1 pmol/ μ g protein (Table 2).

313

314 3.5. HIU hydrolysis activity of recombinant skate TTR and recombinant rainbow trout HIUHase

315 As the production of HIU, a substrate for HIUHase, reached a peak at 2.4 min after the addition of
316 uricase into the reaction mixture (Fig. 8), we investigated HIUHase activity from this time point by adding
317 trout HIUHase or skate TTR. Hydrolysis of HIU by the trout HIUHase was clearly detected at the
318 concentration of 4.4 μ g/mL. Activity (difference in absorbance at 312 nm between the samples in the
319 absence and the presence of HIUHase) peaked at 2.4–4.0 min and decreased thereafter. However, there was
320 no significant effect of the skate TTR on the hydrolysis of HIU at the same concentration (Fig. 8).

321

322 3.6. Contents of divalent cations in skate TTR molecule

323 The zinc content measured by using ICP-OES was 4.47–6.25 mol/mol TTR (Table 3). Additionally,
324 nickel and copper were also detected at 0.40 and 0.36–2.29 mol/mol TTR, respectively. The contents of
325 cobalt and iron were below detectable levels. The TTRs purified using Co-resin and hydrophobic
326 interaction chromatography had similar total metal contents, 6.76–7.01 mol/mol TTR. The same fractions
327 on gel chromatography of the cell extract, which were obtained from *E. coli* harboring intact pET3a, did
328 not contain detectable levels of the metals analyzed.

329

330

331 4. Discussion

332 The present study demonstrates that skate TTR is a zinc-dependent TH-binding protein. This feature is

333 supported by the presence of a histidine-rich segment in the N-terminal region, the ability to be purified by
334 metal chelate affinity chromatography, inactivation of T3 binding by EDTA and recovery of T3 binding
335 activity by divalent cations. Skate TTR had high-affinity and low-affinity sites for T3 with K_{ds} of 0.24 nM
336 and 17 nM, but not HIU hydrolysis activity. All of the high affinity and most of the low affinity sites for T3
337 were abolished by the treatment of EDTA. Analysis by IPC-OES revealed that the skate TTR molecule
338 contains 4.47–6.25 zinc ions. Therefore, zinc ion may be essential for the skate TTR to bind T3.

339 We discovered that a histidine-rich segment, HSHGDHH, located in the N-terminal region of skate
340 TTR may act as a natural histidine tag, which facilitated the purification of this protein by Ni-affinity
341 chromatography and may also provide a novel ligand binding assay (TTR pull-down assay) for
342 investigating the ligand interaction. The histidine-rich segments of the skate and lamprey TTRs resemble
343 the zinc-binding motif of metalloproteases (HEXXH or HEXXHXXGXXH/D) (Cerdà-Costa and
344 Gomis-Rüth 2014), but are quite different from the metal-binding motif of metallothionein with
345 cysteine-rich motifs (Vašák and Meloni, 2011). TTR is a homotetramer consisting of a dimer of dimers
346 (subunits A and B, and subunits C and D). As the N-terminal regions of two subunits (A and D, or B and C)
347 are located in the vicinity of the entrance of either hormone binding pocket (Hamilton et al., 1993), the two
348 histidine-rich segments in the N-terminal regions are highly likely to act as a histidine tag comparable with
349 the ordinary 6× histidine-tag. In this study, we do not exclude the possibility of the presence of several
350 binding sites for divalent cations in skate TTR molecule besides the N-terminal region.

351 Divalent cation binding to skate TTR is necessary to elicit strong T3 binding activity that may occur at
352 physiological conditions, in which Zn^{2+} is the best possible candidate cation. [^{125}I]T3 binding to skate TTR
353 was inactivated by EDTA and re-activated by divalent cations in vitro. When skate TTR (264 nM) was
354 pre-treated with EDTA (1 mM) at the molar ratio of 1/3,800, [^{125}I]T3 binding to the skate TTR was
355 partially inhibited. This suggests that most of the zinc ions involved in T3 binding do not dissociate from
356 the TTR of the micromolar range. The concentration of Zn^{2+} that was needed to reactivate the [^{125}I]T3
357 binding activity, ~0.05 mM, was less than the physiological range (0.1–0.2 mM) of Zn^{2+} in fish plasma
358 (Sturrock et al. 2013). Scatchard analysis revealed the presence of two classes of binding sites. [^{125}I]T3
359 binding to all of the high affinity sites and most of the low affinity sites were lost with the addition of 1
360 mM EDTA. This finding leads us to the possibilities that Zn^{2+} binding is essential for skate TTR to express

361 at least high affinity sites for T3 binding and that Zn²⁺ at the concentration in plasma may modulate T3
362 binding to skate TTR in vivo. In this study we determined the average number of metal ions per TTR. If
363 skate TTR samples consist of a mixture of the TTR components with different content of Zn²⁺ or the Zn²⁺
364 content of skate TTR in circulation differs locally, a variety of the number of Zn²⁺ per TTR may increase
365 the functional diversity in T3 binding activity. Future study will need to address the physiological meanings
366 of Zn²⁺ binding to TTR on the skate thyroid system.

367 This is the first report showing the divalent-dependent TH binding activity of TTR, although there are
368 several reports regarding the effects of metal ions on the other functions of human TTR. Zn²⁺ binding
369 decreases monomer stability to enhance TTR aggregation at an acidic pH (Palmieri et al., 2010) or amyloid
370 formation of a mutant TTR (Wilkinson-White and Easterbrook-Smith, 2007), and decreases the affinity of
371 TTR for RBP4 (Palmieri et al., 2010). Zn²⁺ is also essential for expressing the metalloprotease activity of
372 human TTR, which was inhibited by EDTA or 1,10-phenanthroline and reactivated by divalent cations (Liz
373 et al., 2012). Zinc content in human TTR was ~0.2 per TTR molecule (Liz et al., 2012), which was one
374 order less than that in the skate TTR (4.47–6.25 per TTR). In addition, the skate TTR contained copper at
375 0.36–2.29 per TTR, and nickel at 0.4 per TTR. This means that four fifths of human TTR is independent of
376 zinc-dependent functions. However, in the skate TTR, because of the high content of zinc, T3 binding
377 activity which is highly zinc-dependent may be fully affected by the zinc content. Therefore, the deficiency
378 of metal ions such as zinc may influence the functions of TTR to greater extent in skates compared with
379 humans.

380 Zn²⁺ binding may be an ancient property of the TTR/HIUHase superfamily with high diversity. In the
381 TTR family, Zn²⁺ binding is experimentally shown so far in the skate and human protein alone. Among the
382 four Zn²⁺ binding sites (ZBS1 to ZBS4) proposed in human TTR (Palmieri et al., 2010), only ZBS1 (C10
383 and H56 in Fig. 1) is conserved in the vertebrate TTRs investigated. Among ten amino acid residues that
384 constitute the four Zn²⁺ binding sites in the human TTR, four are identical and one is similar to the
385 corresponding amino acid residues in the skate TTR. The histidine-rich segments found in the skate and
386 lamprey TTRs are not detected in the bony fish and tetrapod TTRs (Fig.1) or HIUHases of various
387 vertebrates. However, in the HIUHase family, our previous study (Kasai et al., 2013) showed that Zn²⁺ (50
388 μM) inhibits significantly the HIU hydrolysis activity of rainbow trout HIUHase. The protein structure of *E.*

389 *coli* HIUHase revealed the presence of zinc ions bound to the functional sites (Lundberg et al., 2006). All
390 of these circumstances suggest that Zn²⁺ binding may be a common property of the HIUHase/TTR
391 superfamily. Interestingly, the number of histidine residues in TTR polypeptide has changed during
392 vertebrate evolution: 11 for lamprey and skate, 7–8 for bony fishes, 6 for amphibians, 5 for reptiles and a
393 bird and 4 for humans (Fig. 1). It is likely that TTR has evolved from a strong to weak divalent cation
394 binder (Wang et al., 2013). Although there is no **experimental** data to explain why the histidine content in
395 TTR sequences **is high in lamprey and skate TTRs and** continuously decreased during vertebrate evolution,
396 **some of these histidine residues may participate in divalent cation binding and contribute to the acquisition**
397 **or reinforcement of TH binding activity in an ancestor of the agnathan and cartilaginous fish TTRs** soon
398 after TTR diverged from ancestral HIUHase.

399 Skate TTR showed the highest affinity for T3 among the vertebrate TTRs studied so far, with K_{d1} of
400 10^{-10} M, which is comparable to those of nuclear TH receptors ($K_d=10^{-11}$ – 10^{-10} nM) (Oppenheimer et al.,
401 1996). Giving that plasma TH levels are 10^{-9} – 10^{-8} M in several elasmobranchs: the whitetip reef shark
402 *Triacnodon obesus* (Crow et al., 1999), dogfish *Squalus acanthias* (Leary et al., 1999) and Atlantic stingray
403 *Dasyatis Sabina* (Volkoff et al., 1999), skate TTR may be functional as a T3-binder rather than T4-binder.
404 The preference for T3 over T4 was also detected in bony fish (Kasai et al., 2013; Kawakami et al., 2006;
405 Santos and Power, 1999; Yamauchi et al., 1999), amphibian (Prapunpoj et al., 2000; Yamauchi et al., 1993),
406 reptilian (Prapunpoj et al., 2002) and **bird** (Chang et al., 1999), but not in mammalian TTRs (**Chang et al.,**
407 **1999**), suggesting that TTR has originally evolved as a T3-binder during the early evolution of fish and
408 changed as T4-binder during the early evolution of mammals (**Richardson, 2007; 2015**).

409 We applied the TTR pull-down assay for ligand binding to skate TTR. Ligand preference of TTR
410 tested by this assay agreed well with that tested by the [¹²⁵I]T3 competitive binding assay for endogenous
411 and exogenous ligands. The TTR pull-down assay is a convenient and a non-radioisotopic method that can
412 estimate directly and **semi-quantitatively** the ligand-TTR interaction. Furthermore, the TTR-pull-down
413 assay can detect several potent chemicals with different retention times on HPLC at the same time. The
414 drawback is that relatively high concentrations of ligands and TTR are needed to quantify their amounts by
415 HPLC, and that the accuracy of this assay is not high. Therefore, this assay may be suitable for the primary
416 screening **that allows to estimate semi-quantitatively** environmental contaminants with significant affinity

417 for TTR and with significantly high absorption spectrum in the ultraviolet or visible region.

418 Skate TTR has significant high affinity for several halogenated phenolic compounds that structurally
419 resemble THs (Howdeshell, 2002). Tetrabromobisphenol A and pentabromophenol were the most potent
420 chemicals in halogenated phenolic compounds with two phenolic rings and with a single ring, respectively.
421 The structural preference of ligand binding was well conserved in vertebrate evolution (Kudo et al., 2006;
422 Meerts et al., 2000; Morgado et al., 2007; Yamauchi et al., 2003). Furthermore, in the structure-activity
423 relationships, halogen species-dependency ($\text{Br}^- > \text{Cl}^-$ in pentahalogenated phenols; $\text{I}^- > \text{Br}^- \approx \text{Cl}^-$ in
424 trihalogenated phenols; $\text{Br}^- > \text{Cl}^- > \text{no halogen}$ in bisphenol A) and halogen number-dependency (penta-
425 >tri- in brominated and chlorinated phenols) are similar with previous studies using human (Meerts et al.,
426 2000), chicken and amphibian TTRs (Kudo et al., 2006; Yamauchi et al., 2003).

427 Production of brominated phenols, used as a flame retardant or its intermediate, or as a wood
428 preservative, may result in the release of brominated phenols to the aquatic environment for several
429 decades (WHO, 2005). The annual consumption by humans of tetrabromobisphenol A is 89,400 tons in
430 Asia, which is 56% of the total market demand in 2001 (Birnbaum and Staskal, 2004). As skates spend
431 time in the sediments of the sea, where they feed on various invertebrates including decapod crustaceans,
432 amphipods and polychaete worms, they are ecologically situated in the top or middle of the benthic food
433 web. This ecological position may expose skates to hydrophobic and persistent organic pollutants retained
434 in the benthic environments with a relatively high bioaccumulation. Therefore, investigating the inhibitory
435 effects of persistent halogenated compounds on TH binding to skate TTR may be useful to assess the threat
436 on the thyroid system from environmental chemicals in benthic environments.

437 In conclusion, we have demonstrated that skate TTR is a strong T3-binder in vitro, and that T3
438 binding to skate TTR is divalent cation-dependent and competitively inhibited by environmental phenolic
439 compounds with halogens. The unique structure of a histidine-rich segment in the N-terminal region may
440 act as a natural histidine tag, raising the possibility that the TH binding activity of the skate TTR may be
441 modulated by Zn^{2+} in plasma. We proposed that a histidine-rich segment in the N-terminal region of TTR
442 may play an important role in acquisition or reinforcement of TH binding activity via metal binding during
443 early vertebrate evolution.

444

445 Conflict of interest statement

446 The authors declare that there are no conflicts of interest.

447

448

449 **Acknowledgments**

450 We are grateful to Miss Yuki Oota for her technical assistance of the TTR pull-down assay, and Mrs C. M.
451 Smith, Mount Desert Island Biological Laboratory (Salsbury Cove, ME 04672, USA) for kindly providing
452 the little skate TTR cDNA. We also wish to express our thanks to Dr. J. Monk for a thorough and critical
453 reading of the manuscript. This work was supported in part by Grant-in Aid of Science Research (C)
454 (25340046) from Japan Society for Promotion of Science.

455

456

457 **References**

458 Aldred, A.R., Prapunpoj, P., Schreiber, G., 1997. Evolution of shorter and more hydrophilic transthyretin
459 N-termini by stepwise conversion of exon 2 into intron 1 sequences (shifting the 3' splice site of intron
460 1). *Eur. J. Biochem.* 246, 401-409.

461 Benton, M.J., 2005. *Vertebrate Palaeontology*, 3rd ed. Blackwell, Malden, MA, USA, pp185.

462 Birnbaum, L.S., Staskal, D.F., 2004. Brominated flame retardants: cause for concern? *Environ. Health*
463 *Perspect.* 112, 9-17.

464 Cendron, L., Ramazzina, I., Percudani, R., Rasore, C., Zanotti, G., Berni, R., 2011. Probing the evolution of
465 hydroxyisourate hydrolase into transthyretin through active-site redesign. *J. Mol. Biol.* 409, 504-512.

466 Cerdà-Costa, N., Gomis-Rüth, F.X., 2014. Architecture and function of metallopeptidase catalytic domains.
467 *Protein Sci.* 23, 123-144.

468 Chang, L., Munro, S.L., Richardson, S.J., Schreiber, G., 1999. Evolution of thyroid hormone binding by
469 transthyretins in birds and mammals. *Eur. J. Biochem.* 259, 534-542.

470 Crow, G.L., Ron, B., Atkinson, S., Rasmussen, L.E.L., 1999. Serum T4 and serum T3 concentrations in
471 immature captive whitetip reef sharks, *Triaenodon obesus*. *J. Exp. Zool.* 284, 500-504.

472 Cyr, D.G., Eales, J.G., 1992. Effects of short-term 17 β -estradiol treatment on the properties of T4-binding

473 proteins in the plasma of immature rainbow trout, *Oncorhynchus mykiss*. J. Exp. Zool. 262, 414-419.

474 Duan, W., Achen, M.G., Richardson, S.J., Lawrence, M.C., Wettenhall, R.E., Jaworowski, A., Schreiber,
475 G., 1991. Isolation, characterization, cDNA cloning and gene expression of an avian transthyretin.
476 Implications for the evolution of structure and function of transthyretin in vertebrates. Eur. J. Biochem.
477 200, 679-687.

478 Hamilton, J.A., Steinrauf, L.K., Braden, B.C., Liepnieks, J., Benson, M.D., Holmgren, G., Sandgren, O.,
479 Steen, L., 1993. The x-ray crystal structure refinements of normal human transthyretin and the
480 amyloidogenic Val-30→Met variant to 1.7-Å resolution. J. Biol. Chem. 268, 2416-2424.

481 **Howdeshell, K.L., 2002. A model of the development of the brain as a construct of the thyroid system.**
482 **Environ. Health Perspect. 110 Suppl , 337-348.**

483 Jain, S., Sharma, S., Gupta, M.N., 2002. A microassay for protein determination using microwaves. Anal.
484 Biochem. 311, 84-86.

485 Kanda, Y., Goodman, D.S., Canfield, R.E., Morgan, F.J., 1974. The amino acid sequence of human plasma
486 prealbumin. J. Biol. Chem. 249, 6796-6805.

487 Kasai, K., Nishiyama, N., Yamauchi, K., 2013. Characterization of *Oncorhynchus mykiss*
488 5-hydroxyisourate hydrolase/transthyretin superfamily: evolutionary and functional analyses. Gene 531,
489 326-336.

490 Kawakami, Y., Seoka, M., Miyashita, S., Kumai, H., Ohta, H., 2006. Characterization of transthyretin in
491 the Pacific bluefin tuna, *Thunnus orientalis*. Zoolog. Sci. 23, 443-448.

492 Kudo, Y., Yamauchi, K., Fukazawa, H., Terao, Y., 2006. In vitro and in vivo analysis of the thyroid
493 system-disrupting activities of brominated phenolic and phenol compounds in *Xenopus laevis*. Toxicol.
494 Sci. 92, 87-95.

495 Laemmli, U.K., 1970. Cleavage of structural proteins during the assembly of the head of bacteriophage T4.
496 Nature 227, 680-685.

497 Leary, S.C., Ballantyne, J.S., Leatherland, J.F., 1999. Evaluation of thyroid hormone economy in
498 elasmobranch fishes, with measurements of hepatic 5'-monodeiodinase activity in wild dogfish. J. Exp.
499 Zool. 284, 492-499.

500 Lee, Y., Lee, D.H., Kho, C.W., Lee, A.Y., Jang, M., Cho, S., Lee, C.H., Lee, J.S., Myung, P.K., Park, B.C.,

501 Park, S.G., 2005. Transthyretin-related proteins function to facilitate the hydrolysis of
502 5-hydroxyisourate, the end product of the uricase reaction. *FEBS Lett.* 579, 4769-4774.

503 Li, Z., Yao, F., Li, M., Zhang, S., 2013. Identification and bioactivity analysis of transthyretin-like protein
504 in amphioxus: a case demonstrating divergent evolution from an enzyme to a hormone distributor.
505 *Comp. Biochem. Physiol. B Biochem. Mol. Biol.* 164, 143-150.

506 Liz, M.A., Leite, S.C., Juliano, L., Saraiva, M.J., Damas, A.M., Bur, D., Sousa, M.M., 2012. Transthyretin
507 is a metallopeptidase with an inducible active site. *Biochem. J.* 443, 769-778.

508 Lundberg, E., Bäckström, S., Sauer, U.H., Sauer-Eriksson, A.E., 2006. The transthyretin-related protein:
509 structural investigation of a novel protein family. *J. Struct. Biol.* 155, 445-457.

510 Manzon, R.G., Neuls, T.M., Manzon, L.A., 2007. Molecular cloning, tissue distribution, and developmental
511 expression of lamprey transthyretins. *Gen. Comp. Endocrinol.* 151, 55-65.

512 Meerts, I.A., van Zanden, J.J., Luijckx, E.A., van Leeuwen-Bol, I., Marsh, G., Jakobsson, E., Bergman, A.,
513 Brouwer, A., 2000. Potent competitive interactions of some brominated flame retardants and related
514 compounds with human transthyretin in vitro. *Toxicol. Sci.* 56, 95-104.

515 Morgado, I., Hamers, T., Van der Ven, L., Power, D.M., 2007. Disruption of thyroid hormone binding to
516 sea bream recombinant transthyretin by ioxinyl and polybrominated diphenyl ethers. *Chemosphere* 69,
517 155-163.

518 Oppenheimer, J.H., Schwartz, H.L., Strait, K.A., 1996. The molecular basis of thyroid hormone actions. In:
519 Braverman, L.E., Utiger, R.D. (Eds.), *Werner and Ingbar's the Thyroid*. 7th ed. Lippincott-Raven,
520 Philadelphia, pp. 162-184.

521 Palmieri Lde, C., Lima, L.M., Freire, J.B., Bleicher, L., Polikarpov, I., Almeida, F.C., Foguel, D., 2010.
522 Novel Zn²⁺-binding sites in human transthyretin: implications for amyloidogenesis and retinol-binding
523 protein recognition. *J. Biol. Chem.* 285, 31731-31741.

524 Prapunpoj, P., Leelawatwatana, L., Schreiber, G., Richardson, S.J., 2006. Change in structure of the
525 N-terminal region of transthyretin produces change in affinity of transthyretin to T4 and T3. *FEBS J.*
526 273, 4013-4023.

527 Prapunpoj, P., Richardson, S.J., Schreiber, G., 2002. Crocodile transthyretin: structure, function, and
528 evolution. *Am. J. Physiol. Regul. Integr. Comp. Physiol.* 283, R885-R896.

529 Prapunpoj, P., Yamauchi, K., Nishiyama, N., Richardson, S.J., Schreiber, G., 2000. Evolution of structure,
530 ontogeny of gene expression, and function of *Xenopus laevis* transthyretin. Am. J. Physiol. Regul.
531 Integr. Comp. Physiol. 279, R2026-R2041.

532 Ramazzina, I., Folli, C., Secchi, A., Berni, R., Percudani, R., 2006. Completing the uric acid degradation
533 pathway through phylogenetic comparison of whole genomes. Nat. Chem. Biol. 2, 144-148.

534 Richardson, S.J., 2007. Cell and molecular biology of transthyretin and thyroid hormones. Int. Rev. Cytol.
535 258, 137-193.

536 Richardson, S.J., 2015. Tweaking the structure to radically change the function: the evolution of
537 transthyretin from 5-hydroxyisourate hydrolase to triiodothyronine distributor to thyroxine distributor.
538 Front. Endocrinol. (Lausanne) 5, 245.

539 Richardson, S.J., Monk, J.A., Shepherdley, C.A., Ebbesson, L.O., Sin, F., Power, D.M., Frappell, P.B.,
540 Köhrle, J., Renfree, M.B., 2005. Developmentally regulated thyroid hormone distributor proteins in
541 marsupials, a reptile, and fish. Am. J. Physiol. Regul. Integr. Comp. Physiol. 288, R1264-R1272.

542 Robbins, J., 1996. Thyroid hormone transport proteins and the physiology of hormone binding. In:
543 Braverman, L.E., Utiger, R.D. (Eds.), Werner and Ingbar's the Thyroid. 7th ed. Lippincott-Raven,
544 Philadelphia, pp. 96-110.

545 Rosenthal, H.E., 1967. A graphic method for the determination and presentation of binding parameters in a
546 complex system. Anal. Biochem. 20, 525-532.

547 Santos, C.R., Power, D.M., 1999. Identification of transthyretin in fish (*Sparus aurata*): cDNA cloning and
548 characterisation. Endocrinology 140, 2430-2433.

549 Scatchard, G., 1949. The attractions of proteins for small molecules and ions. Ann. NY Acad. Sci. 51,
550 660-672.

551 Sturrock, A.M., Hunter, E., Milton, J.A., Trueman, C.N., 2013. Analysis methods and reference
552 concentrations of 12 minor and trace elements in fish blood plasma. J. Trace Elem. Med. Biol. 27,
553 273-285.

554 Vašák, M., Meloni, G., 2011. Chemistry and biology of mammalian metallothioneins. J. Biol. Inorg. Chem.
555 16, 1067-1078.

556 Volkoff, H., Wourms, J.P., Amesbury, E., Snelson, F.F., 1999. Structure of the thyroid gland, serum

557 thyroid hormones, and the reproductive cycle of the Atlantic stingray, *Dasyatis sabina*. J. Exp. Zool.
558 284, 505-516.

559 Wang, F., Chmil, C., Pierce, F., Ganapathy, K., Gump, B.B., MacKenzie, J.A., Metchref, Y., Bendinskas,
560 K., 2013. Immobilized metal affinity chromatography and human serum proteomics. J. Chromatogr. B
561 Analyt. Technol. Biomed. Life Sci. 934, 26-33.

562 WHO (World Health Organization), 2005. 2,4,5-Tribromophenol and other simple brominated phenols.
563 Concise International Chemical Assessment Document 66, WHO, Geneva.

564 Wilkinson-White, L.E., Easterbrook-Smith, S.B., 2007. Characterization of the binding of Cu(II) and Zn(II)
565 to transthyretin: effects on amyloid formation. Biochemistry 46, 9123-9132.

566 Yamauchi, K., Ishihara, A., Fukazawa, H., Terao, Y., 2003. Competitive interactions of chlorinated phenol
567 compounds with 3,3',5-triiodothyronine binding to transthyretin: detection of possible
568 thyroid-disrupting chemicals in environmental waste water. Toxicol. Appl. Pharmacol. 187, 110-117.

569 Yamauchi, K., Kasahara, T., Hayashi, H., Horiuchi, R., 1993. Purification and characterization of a
570 3,5,3'-L-triiodothyronine-specific binding protein from bullfrog tadpole plasma: a homolog of
571 mammalian transthyretin. Endocrinology 132, 2254-2261.

572 Yamauchi, K., Nakajima, J., Hayashi, H., Hara, A., 1999. Purification and characterization of
573 thyroid-hormone-binding protein from masu salmon serum. A homolog of higher-vertebrate
574 transthyretin. Eur. J. Biochem. 265, 944-949.

575 Yamauchi, K., Takeuchi, H., Overall, M., Dziadek, M., Munro, S.L., Schreiber, G., 1998. Structural
576 characteristics of bullfrog (*Rana catesbeiana*) transthyretin and its cDNA--comparison of its pattern of
577 expression during metamorphosis with that of lipocalin. Eur. J. Biochem. 256, 287-296.

578 Yancey, P.H., 2005. Organic osmolytes as compatible, metabolic and counteracting cytoprotectants in high
579 osmolarity and other stresses. J. Exp. Biol. 208, 2819-2830.

580 Zanotti, G., Cendron, L., Ramazzina, I., Folli, C., Percudani, R., Berni, R., 2006. Structure of zebra fish
581 HIUase: insights into evolution of an enzyme to a hormone transporter. J. Mol. Biol. 363, 1-9.

582

583

584

585 **Figure legends**

586 Fig. 1. Comparison of transthyretin (TTR) sequences with possible zinc-binding sites. Mature TTR amino
587 acid sequences from lamprey (Manzon et al., 2007), skate (accession no. CV221819), trout (Yamauchi et
588 al., 1999; accession.no.CX256523), seabream (Santos and Power, 1999), toad (Prapunpoj et al., 2000),
589 bullfrog (Yamauchi et al., 1993, 1998), crocodile (Prapunpoj et al., 2002), chicken (Duan et al., 1991) and
590 human (Kanda et al., 1974) were aligned. The N-terminal ends of the lamprey, skate and seabream TTRs
591 are predicted, whereas those of the other TTRs are based on Edman degradation. The numbering of amino
592 acid is based on that of human TTR. Features of secondary structure of human TTR (Hamilton et al., 1993)
593 are indicated above the lamprey sequence. Histidine-rich segments in the disordered N-terminal region of
594 the skate and lamprey TTRs are boxed. A segment that resembles a zinc-binding motif of metalloprotease
595 (HEXXHXXGCCCH/D) (Cerdà-Costa and Gomis-Rüth, 2014) is underlined. Four zinc-binding sites (ZBSs
596 1-4) proposed in human TTR (Palmieri et al., 2010) are also boxed: C10 and H56 for ZBS1, H88, H90 and
597 E92 for ZBS2, H31, D74 and E72 (or E62 at acidic pH), H31, E61 and D74 for ZBS4. Marks (*)
598 underneath the sequence alignment indicate positions where amino acid residues are invariant, among the 9
599 sequences. The numbers of histidine residues in the TTR sequences are shown on the right.

600

601 Fig. 2. Purification of recombinant skate transthyretin (TTR) by metal chelate affinity chromatography and
602 gel chromatography. (A) SDS-PAGE of the fractions of metal chelate affinity chromatography. The
603 recombinant skate TTR was separated from the other bacterial proteins in cell extract by metal chelate
604 affinity chromatography on Ni-resin, and then eluted with the buffer containing 150 mM imidazole (*an*
605 *arrow* in fraction *E4*). Lanes from left to right: *ppt*, pellet of cell lysate; *sup*, supernatant of cell lysate; *FT*,
606 flow-through fraction; *W1* to *W4*, washing fractions; *E1* to *E6*, elution fractions with buffer containing 5, 20,
607 60, 150, 250, 500 mM imidazole, respectively. (B) High performance gel chromatography of purified
608 recombinant skate TTR. Protein was applied to YMC Diol 120 High performance gel chromatography
609 column (8 × 500 mm) in 50 mM Tris-HCl, pH 7.5, and 140 mM NaCl, at 1 mL/min. **Elution was monitored**
610 **at absorbance at 280 nm**. Markers: Blue dextran (void volume, V_0); apoferritin (Fer, 440 kDa); alcohol
611 dehydrogenase (ADH, 158 kDa); bovine serum albumin (BSA, 68 kDa); ovalbumin (OVA, 45 kDa); and
612 myoglobin (Mb, 17 kDa). (C) SDS-PAGE of the peak fraction of Cellulofine GCL-2000 sf gel filtration

613 chromatography. *Arrow*, band of skate TTR.

614

615 Fig. 3. Ligand-binding to recombinant skate transthyretin (TTR) determined by the TTR pull-down assay
616 using metal chelate affinity resin. After incubating TTR (14.2 µg, 0.5 µM) with each ligand (0.5 µM) (A,
617 iodothyronines and their acetic acid analogs; B, environmental chemicals) in 500 µL of the incubation
618 buffer, the ligand bound to TTR was analyzed by reverse phase-HPLC as described in the Materials and
619 methods. The vertical axis of graphs indicates the amount of the bound ligand that was recovered in 40 µL
620 of the extraction buffer. Blank data obtained from samples in the absence of TTR were subtracted from
621 those obtained from samples in the presence of TTR. Each value is the mean ± standard error of the mean
622 ($n = 5-6$ for *panel A*; $n = 3$ for *panel B*). Different letters indicate significantly different means ($p < 0.01$). T3,
623 3,3',5-triiodo-L-thyronine; T4, L-thyroxine; Triac, 3,3',5-triiodothyroacetic acid; Tetrac,
624 3,3',5,5'-tetraiodothyroacetic acid; rT3, 3,3',5'-triiodo-L-thyronine, T2, 3,5-diiodo-L-thyronine, D-T3,
625 3,3',5-triiodo-D-thyronine, TIP, 2,4,6-triiodophenol, 2,4-DNP, 2,4-dinitrophenol.

626

627 Fig. 4. Effects of ethylenediaminetetraacetic acid (EDTA) and divalent cations on [¹²⁵I]T3 binding to
628 recombinant skate transthyretin (TTR). (A) Effect of divalent cations of [¹²⁵I]T3 binding to skate TTR. TTR
629 (0.53 nM) was incubated with 0.1 nM [¹²⁵I]T3 in the presence or absence (control) of 1 mM each divalent
630 cation for 1 h at 4°C. (B) Effect of pre-treatment of TTR at various concentrations with 1 mM EDTA on
631 [¹²⁵I]T3 binding. TTR (0.53–2640 nM) was pre-incubated with or without (control) 1 mM EDTA for 30 min
632 for 4°C. After dilution 1, 5, 50, 500, or 5,000 times with the buffer, TTR (0.53 nM) was incubated with 0.1
633 nM [¹²⁵I]T3 for 1 h at 4°C. (C) Effects of divalent cations on [¹²⁵I]T3 binding to the TTR pre-treated with
634 EDTA. TTR (26.4 nM) was pre-incubated with or without (control) 1 mM EDTA for 30 min for 4°C. After
635 dilution 50 times with the buffer (final concentration of EDTA = 0.02 mM), TTR (0.53 nM) was incubated
636 with 0.1 nM [¹²⁵I]T3 in the presence or absence of 1 mM of each cation for 1 h at 4°C. Binding activity of
637 the TTR that was treated with neither EDTA nor cation (*EDTA-*, *cation -*) is indicated as the control (100%).
638 (D). Zn²⁺-dependent activation of [¹²⁵I]T3 binding to TTR. TTR (26.4 nM) was pre-incubated with 1 mM
639 EDTA for 30 min for 4°C. After dilution 50 times with the buffer, TTR (0.53 nM) was incubated with 0.1
640 nM [¹²⁵I]T3 in various concentrations of Zn²⁺ for 1 h at 4°C. [¹²⁵I]T3 binding activity of the TTR that was

641 untreated with 1 mM EDTA (*open circle*) is indicated as control 100%. Each value is the mean \pm standard
642 error of the mean of triplicate determinations. Experiments were repeated two or three times. Asterisks
643 indicate significant differences in T3 binding activity between the reference sample [cation (-) in *panel A*;
644 EDTA (-) in *panel B*; EDTA(+) and cation (-) in *panels C and D*] and each test sample. *, $p < 0.05$; **,
645 $p < 0.01$.

646

647 Fig. 5. Competition of iodothyronines and their related compounds for [125 I]T3 binding to recombinant
648 skate transthyretin (TTR). TTR (0.53 nM) was incubated with 0.1 nM [125 I]T3 for 1 h at 4°C, in the
649 presence or absence (control) of increasing concentrations of the following compounds:
650 3,3',5-triiodothyroacetic acid (Triac), T3, D-T3, 3,3',5,5'-tetraiodothyroacetic acid (Tetrac), T4, reverse T3
651 (rT3), 3,5-diiodo-L-thyronine (T2), 3,5-diiodo-L-tyrosine (Y2) and 3-iodo-L-tyrosine (Y1). Non-specific
652 binding, which was 3–4 % of total binding, was subtracted from total binding to give values for specific
653 binding. Each value is the mean of triplicate determinations. These experiments were repeated at least three
654 times.

655

656 Fig. 6. Inhibition of [125 I]T₃ binding to recombinant skate transthyretin (TTR) by various environmental
657 chemicals. (A) TTR (0.53 nM) was incubated with 0.1 nM [125 I]T₃ in the presence of 1 μ M of each
658 chemicals or solvent (dimethylsulfoxide, control) for 1 h at 4°C. Asterisks indicate significantly differences
659 in [125 I]T₃ binding activity between control and test samples containing each environmental chemical (**,
660 $p < 0.01$). (B) TTR (0.53 nM) was incubated with 0.1 nM [125 I]T₃ for 1 h at 4°C, in the presence or absence
661 (control) of increasing concentrations of the following compounds: pentabromophenol (PBP), triiodophenol
662 (TIP), pentachlorophenol (PCP), tetrabromobisphenol A (Br4-BPA), tetrachlorobisphenol A (Cl4-BPA),
663 ioxynil, tribromophenol (TBP) and trichlorophenol (TCP). To estimate the relative potency of the test
664 chemicals against T3, the competition curve for unlabeled T3 (broken line) was inserted. Non-specific
665 binding, which was less than 6% of total binding, was subtracted from total binding to give values for
666 specific binding. Each value is the mean of triplicate determinations. These experiments were repeated at
667 least three times.

668

669 Fig. 7. Scatchard plots of [¹²⁵I]T3 binding to recombinant skate transthyretin (TTR). For high-affinity and
670 low affinity sites, TTR was incubated with 0.1 nM [¹²⁵I]T3 M in the presence or absence of various
671 concentrations of unlabeled excess T3 (5 μM) in the incubation buffer with (●; 5.3 nM TTR) or without (○;
672 0.53 nM TTR) 1 mM EDTA for 1 h at 4°C. For high-affinity sites, TTR (0.53 nM) was incubated with
673 [¹²⁵I]T3 ranging from 0.05 to 0.4 nM in the presence or absence of unlabeled excess T3 (5 μM) in the
674 incubation buffer for 1 h at 4°C (*inset*). Non-specific binding, which was 12–16% of total binding, was
675 subtracted from total binding to give values for specific binding. Each value is the mean of triplicate
676 determinations. These experiments were repeated three or four times. v, molar ratio of bound [¹²⁵I]T3 to
677 TTR concentration.

678

679 Fig. 8. Time course of enzyme-dependent 5-hydroxyisourate (HIU) hydrolysis by recombinant rainbow
680 trout 5-hydroxyisourate hydrolase (HIUHase) and recombinant skate transthyretin (TTR). HIUHase, TTR
681 and blank (buffer) were added to the reaction solution containing HIU (*arrow*). The hydrolysis of HIU was
682 monitored spectrophotometrically at 312 nm as described in the Materials and Methods. Enzyme-dependent
683 HIU hydrolysis indicates the difference in absorbance at 312 nm between the samples in the absence
684 (spontaneous degradation of HIU) and the presence of HIUHase or TTR (spontaneous + enzymatic
685 degradation of HIU). These experiments were repeated at least three times, with similar results.

Table 1. Relative potency of ligand binding to skate transthyretin.

Compounds	IC ₅₀ ± SEM (n)			Relative potency*
	(nM)			
3,3',5-Triiodo-L-thyronine	2.0 ± 0.1	(3)	a,b**	1
L-Thyroxine	26 ± 5	(3)	d	0.078
3,3',5'-Triiodo-L-thyronine	81 ± 6	(3)	e	0.025
3,3',5-Triiodo-D-thyronine	4.4 ± 0.3	(3)	b,c	0.46
3,3',5-Triiodothyroacetic acid	1.0 ± 0.2	(3)	a	2.0
3,3',5,5'-Tetraiodothyroacetic acid	9.7 ± 0.8	(3)	c	0.21
3,5-Diiodo-L-thyronine	250 ± 60	(3)	f	0.008
3,5-Diiodo-L-tyrosine	1000 >>	(3)		
3-Doiodo-L-tyrosine	1000 >>	(3)		
Tetrachlorobisphenol A	27 ± 5	(4)	d,e,f,g	0.074
Tetrabromobisphenol A	9.8 ± 2.3	(4)	c,d,e	0.20
Pentachlorophenol	5.1 ± 0.5	(3)	b,c	0.39
Pebtabromophenol	1.4 ± 0.3	(4)	a	1.4
Triiodophenol	2.2 ± 0.4	(3)	a,b	0.91
Tribromphenol	49 ± 11	(3)	g	0.04
Trichlorophenol	44 ± 8	(3)	f,g	0.05
Ioxynil	33 ± 6	(3)	e,f,g	0.06

*Relative potency is given as the ratio of IC₅₀ for T3 to IC₅₀ for a chemical.

**Different letters indicate significantly different means and were determined by one-way analysis of variance with Scheffe's test for multiple comparisons ($p < 0.01$).

Table 2. Kinetic parameters of T3 binding to the recombinant little skate transthyretin.

Chelator	Class	K_d (nM)	MBC (pmol/ μ g protein)
(-) EDTA	two classes (high affinity site)	0.52 ± 0.03 (4)	2.2 ± 1.0 (4)
	(low affinity site)	17 ± 3 (4)	19 ± 5 (4)
	one class (high affinity site)	0.24 ± 0.04 (4)	3.7 ± 1.1 (4)
(+) EDTA	one class	21 ± 1 (3)	1.4 ± 0.1 (3)

Each value is the mean \pm standard error of the mean (n).

Table 3. **Number of** divalent cations in recombinant little skate transthyretin.

	Methods of preparations	
	HIC column	Co-resin
Zn	4.47	6.25
Cu	2.29	0.36
Ni	<0.06	0.40
Co	<0.06	(0.48)
Fe	nd	<0.02
Total metal	6.76	7.01

TTR was prepared by hydrophobic interaction column (HIC) or Co-affinity resin chromatography and then gel filtration chromatography. Data are shown as metal/TTR (mol/mol). Each value is the mean ($n = 3$), with less than 1% variation.

*When Co-affinity chromatography was used, it is likely that the TTR samples were contaminated with Co^{2+} released from the Co-affinity resin. Therefore, these values are not included in the total metal contents.

nd, not determined.

Fig. 2

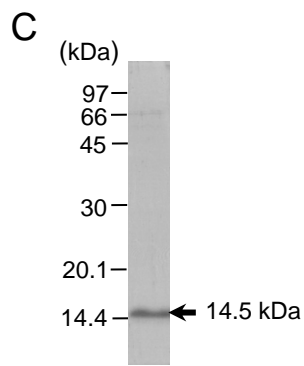
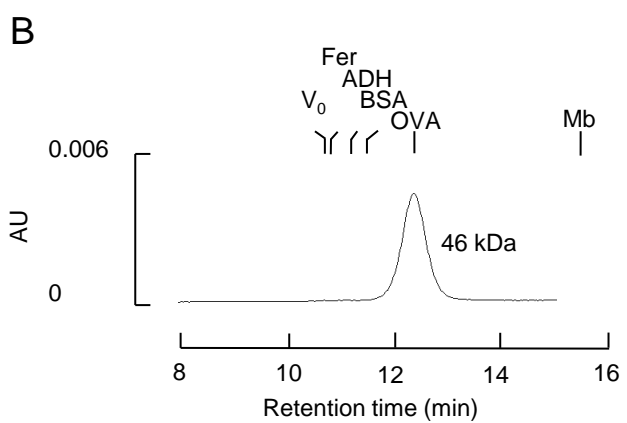
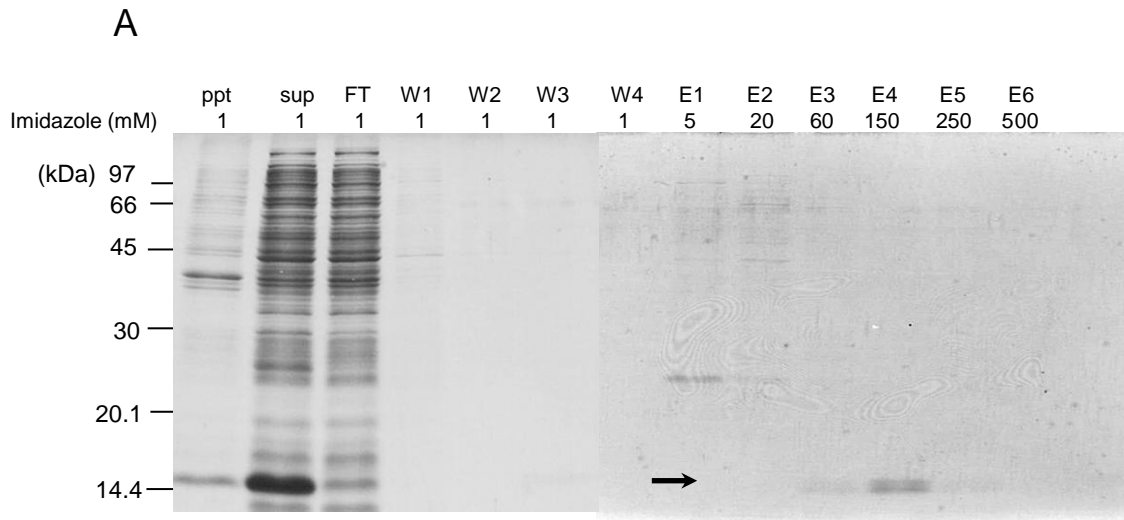


Fig. 3

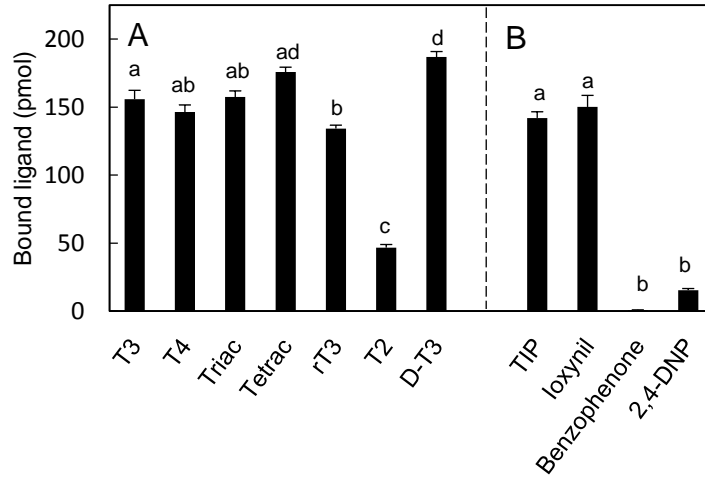


Fig. 4

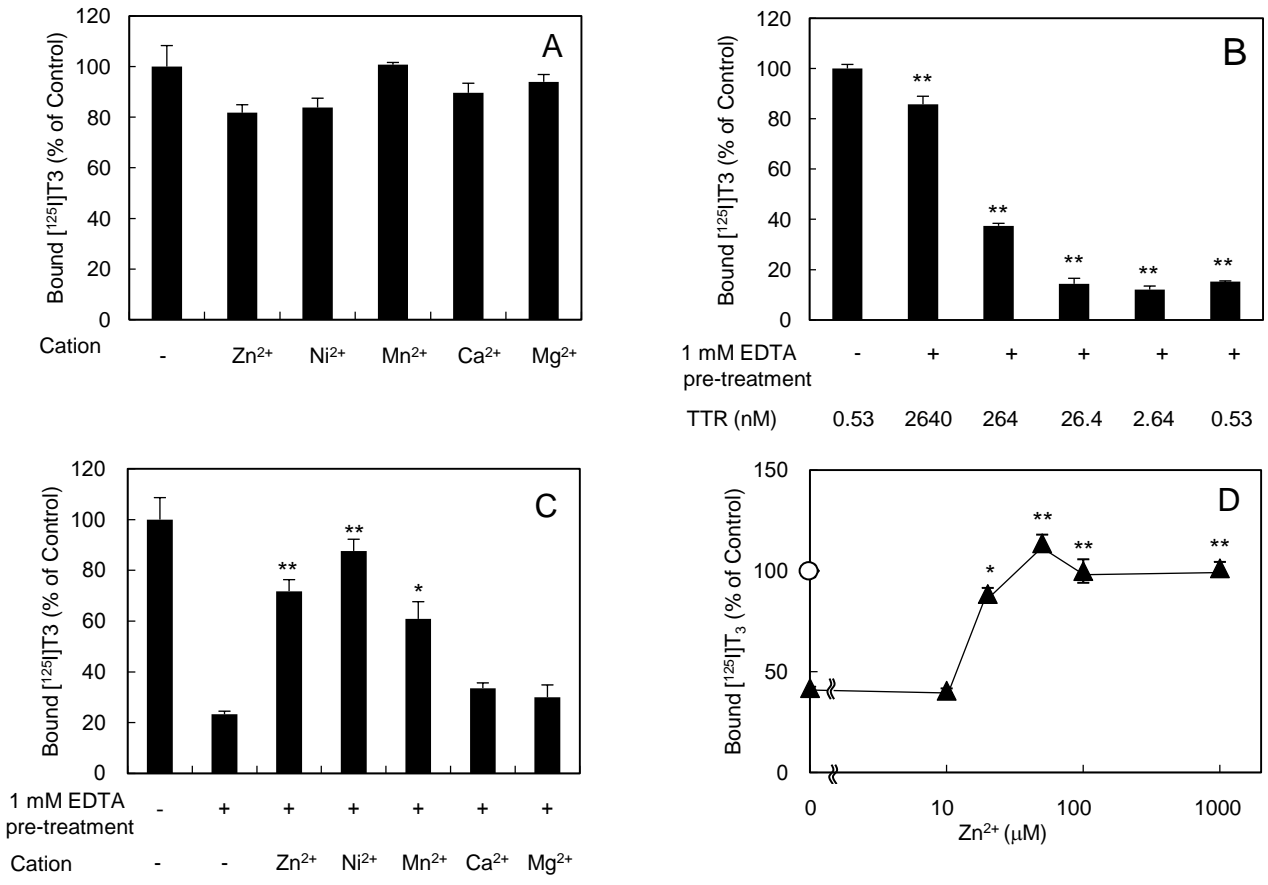


Fig. 5

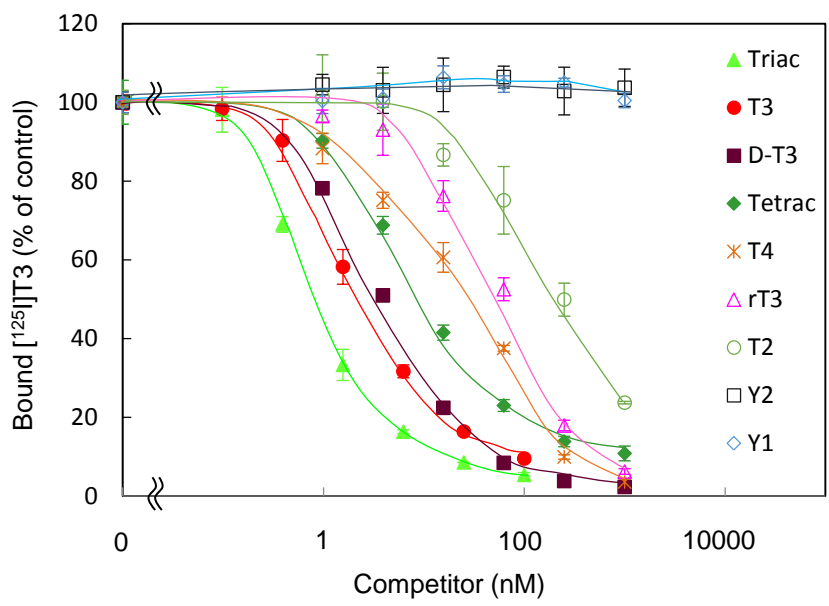
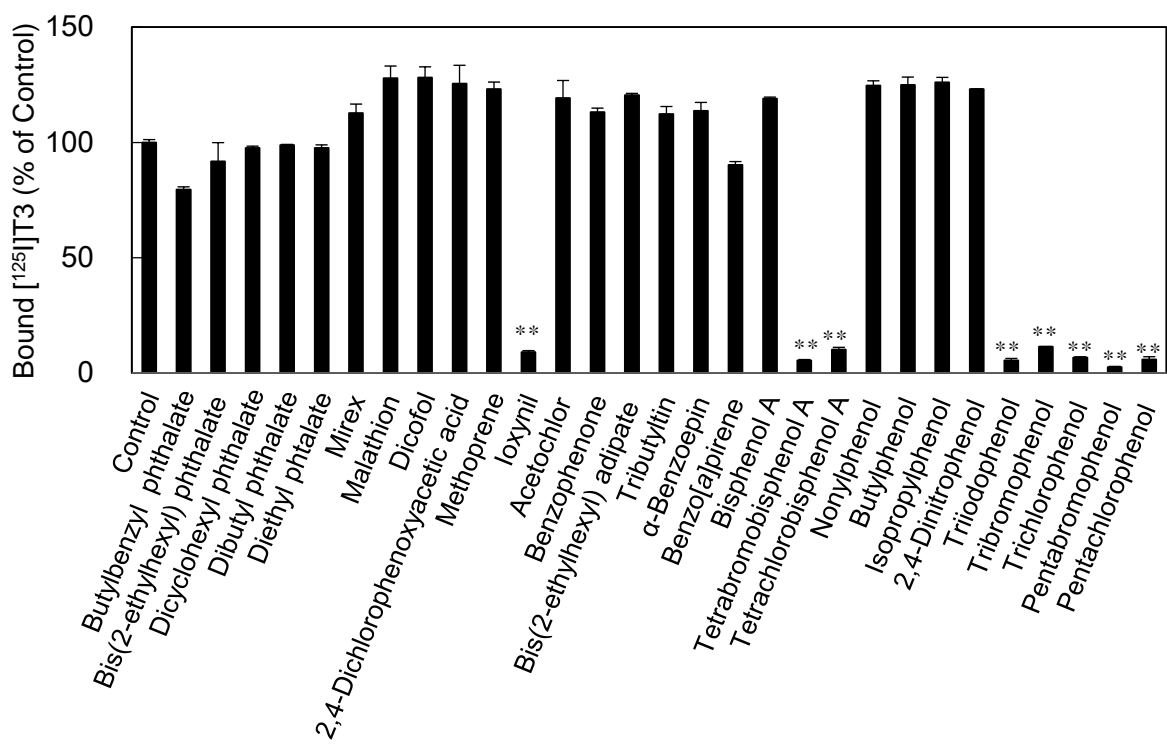


Fig. 6

A



B

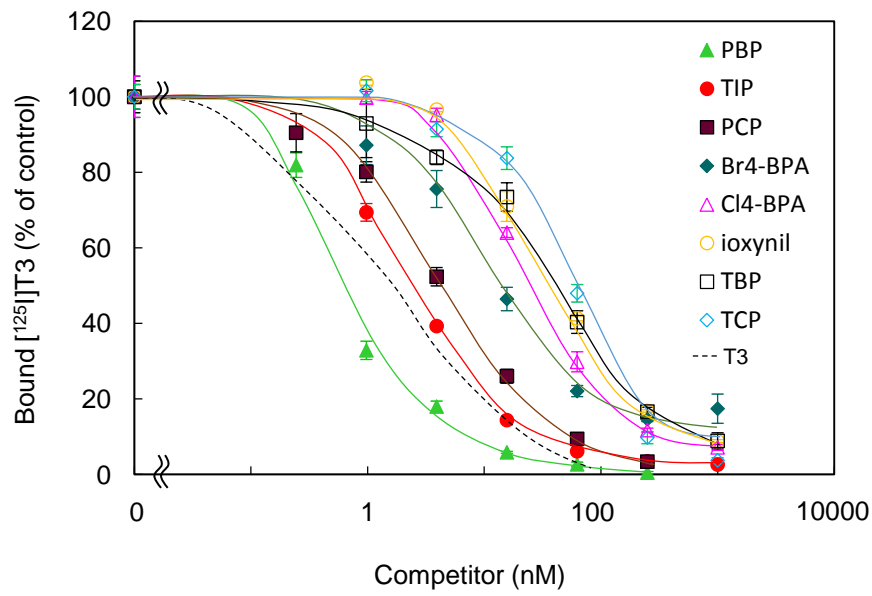


Fig. 7

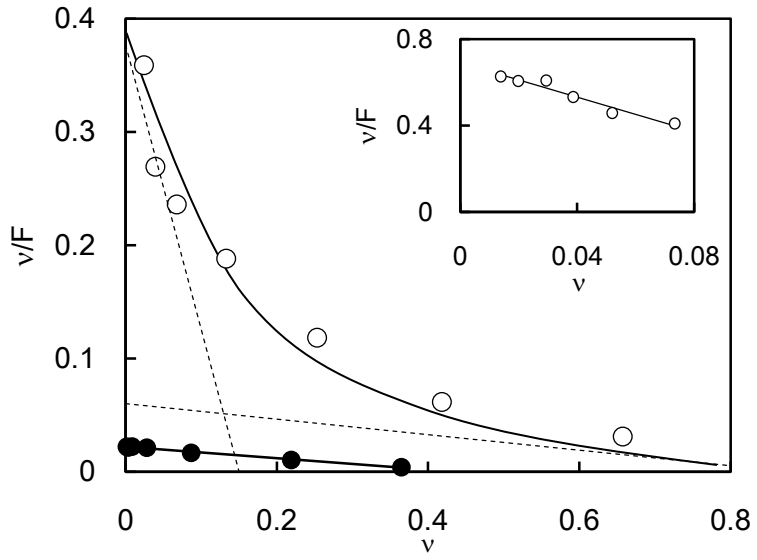
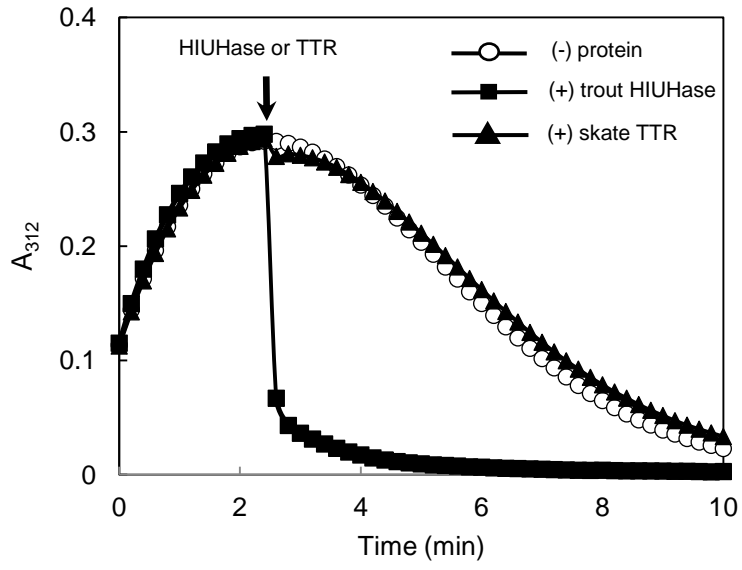


Fig. 8



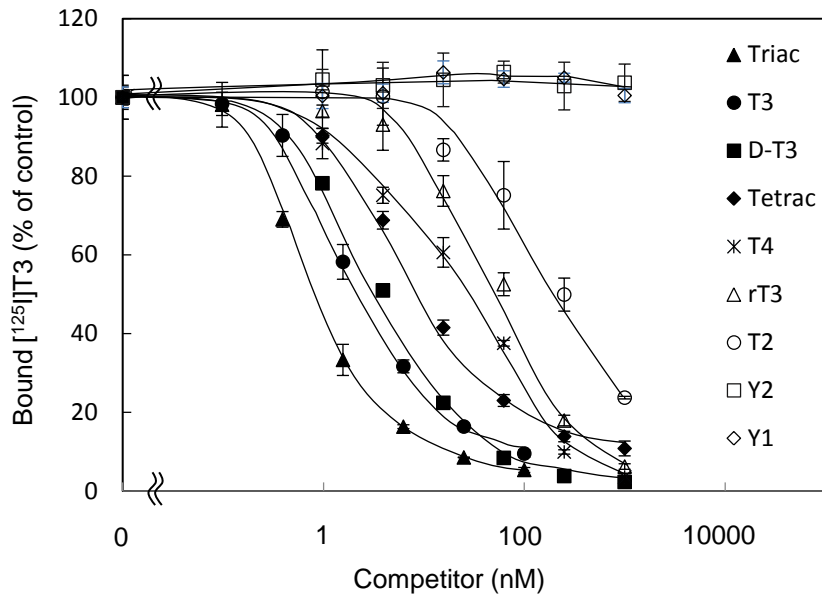
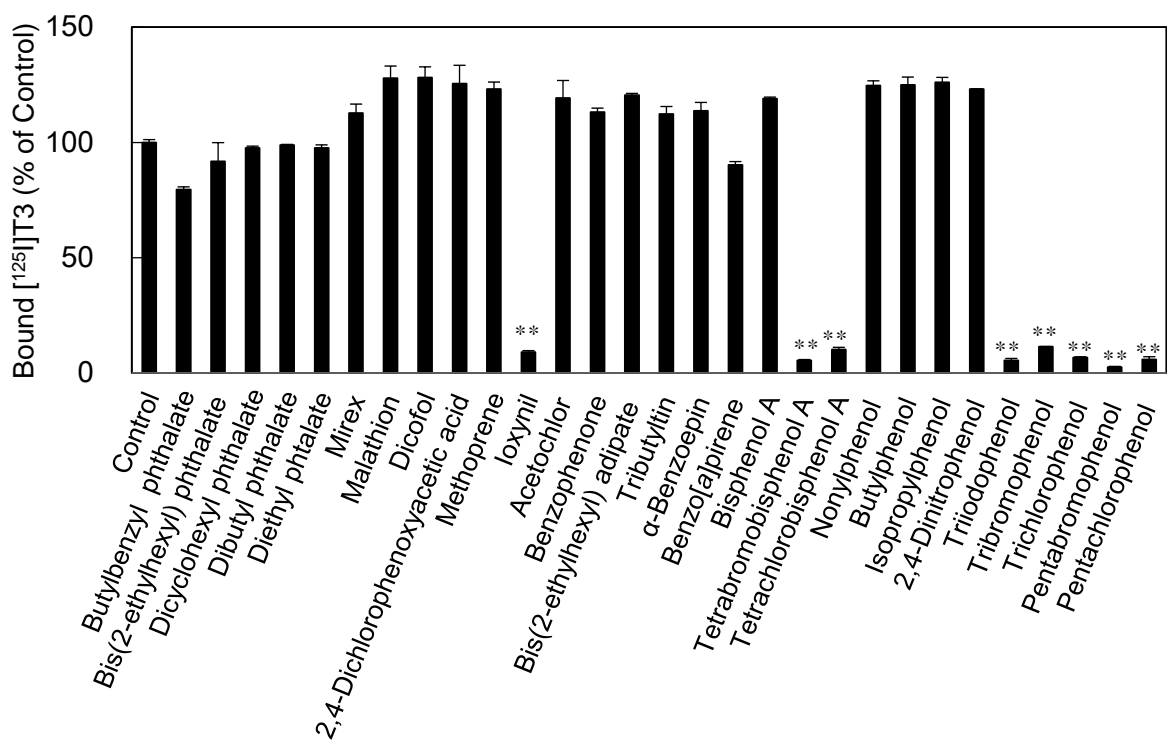


Fig. 6

A



B

